Supporting information

Asymmetric-Structure Design of Electrolyte with Flexibility and Lithium Dendrite-Suppression Ability for Solid-State Lithium Batteries

Huan-Liang Guo,[§,†] Hui Sun,[§,*,†] Zhuo-Liang Jiang,[†] Jian-Yong Hu,[†] Cong-Shan Luo,[†] Meng-Yang Gao,[†] Jing-Yang Cheng,[†] Wen-Ke Shi,[†] Hong-Jun Zhou,[†] Shi-Gang Sun[‡]

[†] State Key Laboratory of Heavy Oil Processing, Beijing Key Laboratory of biogas upgrading utilization, College of New Energy and Materials, China University of Petroleum-Beijing, Fuxue Road No.18, Changping District, Beijing, 102249, China

E-mail: sunhui@cup.edu.cn

[‡] State Key Lab of PCOSS, Xiamen University, Siming South Road No. 422, Xiamen, Fujian province, 361005, China

[§] These authors contributed equally.

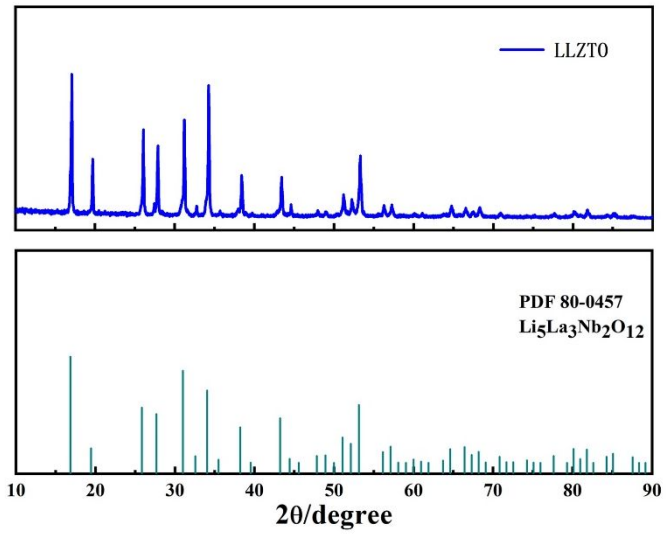

Figure S1. XRD pattern of sintered garnet (LLZTO). Cubic garnet-type $Li_5La_3Nb_2O_{12}$ (PDF 80-0457) is used as the standard XRD pattern to confirm the phase structure of the as-synthesized materials.

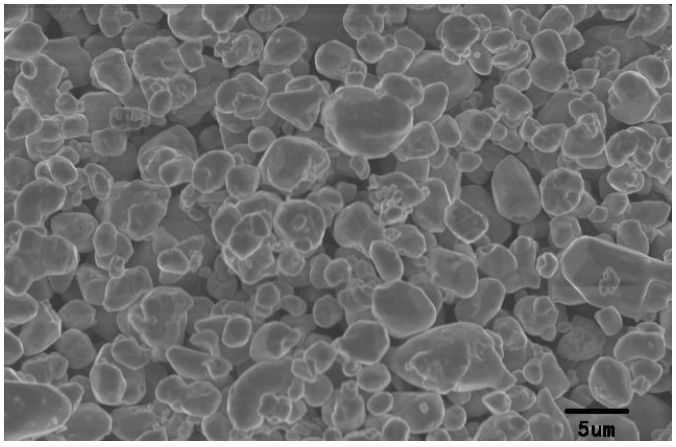

Figure S2. SEM images of the LLZTO ceramic powders.

Figure S3. Photographs of the PEO/LLZTO electrolyte membranes with weight ratio of 1:9.

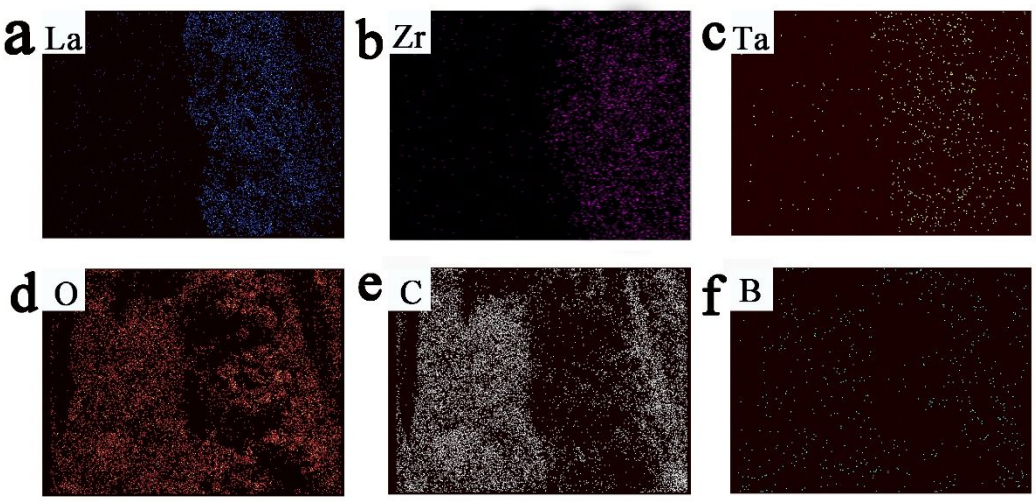

Figure S4. EDS elemental mapping for the cross sections of the ASE, demonstrating a reasonable distribution of La, Zr, Ta, O, C and B elements(a-f) in sample electrolyte.

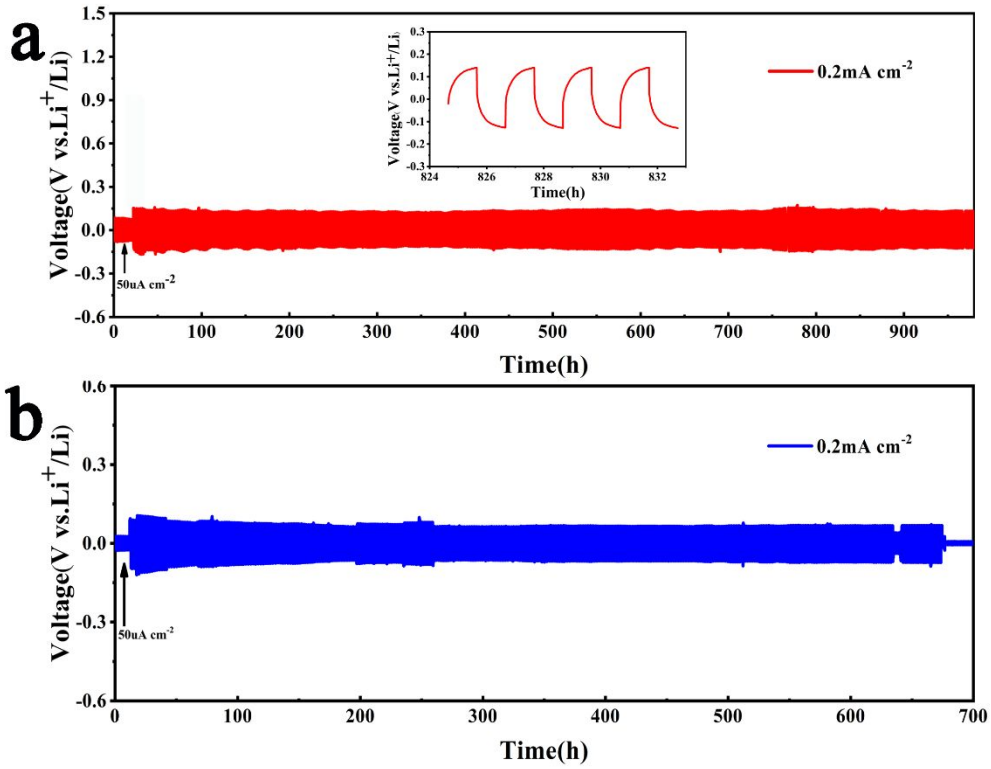

Figure S5. Figure R3 Voltage profiles versus time of Li symmetric cells in the ASE (a) and the SPE (b) at a current density of 0.2 mA cm^{-2}. The inset is the magnified curve.

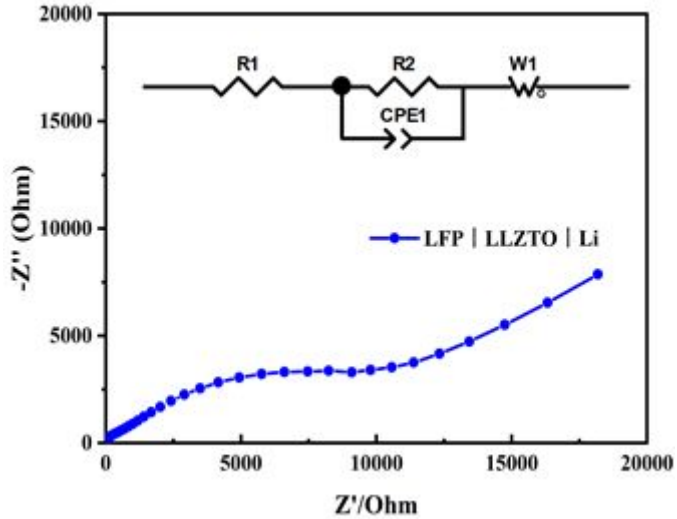

Figure S6. EIS plot of LFP/LLZTO/Li battery. Inset shows the equivalent circuit.

Table S1. Various currents and resistances obtained for the calculation of lithium-ion transference number.

	I_0 (uA)	I_{SS} (uA)	R_0(Ω)	R_{SS} (Ω)	t_{Li+}
Asymmetric solid electrolyte (ASE)	84.89	48.68	82.6	86.7	0.32
PEO-LiBOB electrolyte (SPE)	64.60	25.25	107.5	112.3	0.16

Table S2. The bulk resistance and charge-transfer resistance values for different types SSEs.

	LFP|ASE|Li	LFP|SPE|Li	LFP|ex-situ|Li	LFP|LLZTO|Li
Bulk resistance	35.7	26.13	125.7	1640.2
Charge-transfer resistance	302.8	322.3	2225.0	12258.3

Table S3. Comparing the electrochemical performance of our work with recent publications.

Solid-state electrolyte	Rate	Specific capacity	Number of cycles	Capacity retention	Ref.
PEO/LiBOB- LLZTO/PEO	0.2C	155.1 mAh g^{-1}	200	90.2%	This work
PEO/LiTFSI/LLZTO	0.5C	161.3 mAh g^{-1}	70	97.4%	[1]
PEO/LiTFSI-40wt% LLZTO	0.1C	155 mAh g^{-1}	100	87%	[2]
PEO-n-UIO	0.5C	151 mAh g^{-1}	100	95%	[3]
PEO/LiTFSI-10 wt% LLZTO	0.2C	149.1mAh g^{-1}	100	93.6%	[4]
Li-IL@MOF	0.1C	145 mAh g^{-1}	100	91%	[5]
PEO/BMIMTF$_2$N/LLZTO	0.1C	133.2 mAh g^{-1}	100	84.1%	[6]
PEO/LiTFSI-5%LLTO	0.5C	131 mAh g^{-1}	100	94%	[7]
PVDF-HFP/LLZO/PEC/LiFSI	1.0C	121.4 mAh g^{-1}	100	96.3%	[8]
PEO/LiTFSI-7.5%LLZO	0.5C	121 mAh g^{-1}	100	89%	[9]
PEGMEA/LLZO	0.2C	160.6 mAh g^{-1}	120	94.5%	[10]
PVDF/LLZTO	0.4C	150 mAh g^{-1}	120	98%	[11]
PEGDE-PEGDA-LiTFSI	0.2C	162 mAh g^{-1}	150	77%	[12]
PVDF-HFP/LLZO	0.5C	120 mAh g^{-1}	180	92.5%	[13]
PEC/LiMNT/LiFSI	0.5C	145.9 mAh g^{-1}	200	91.9%	[14]
PEO/LLZTO	0.1C	141.5 mAh g^{-1}	200	90%	[15]
Hierarchical sandwich-type	0.1C	118.6 mAh g^{-1}	200	82.4%	[16]

(1) Wan, Z.; Lei, D.; Yang, W.; Liu, C.; Shi, K.; Hao, X.; Shen, L.; Lv, W.; Li, B.; Yang, Q.-H.; Kang, F.; He, Y.-B. Low Resistance-Integrated All-Solid-State Battery Achieved by $Li_7La_3Zr_2O_{12}$ Nanowire Upgrading Polyethylene Oxide (PEO) Composite Electrolyte and PEO Cathode Binder. *Advanced Functional Materials* **2019,** *29* (1), DOI: 10.1002/adfm.201805301.

(2) Zhao, C. Z.; Zhang, X. Q.; Cheng, X. B.; Zhang, R.; Xu, R.; Chen, P. Y.; Peng, H. J.; Huang, J. Q.; Zhang, Q. An anion-immobilized composite electrolyte for dendrite-free lithium metal anodes. *P Natl Acad Sci USA* **2017,** *114* (42), 11069-11074, DOI: 10.1073/pnas.1708489114.

(3) Wu, J. F.; Guo, X. MOF-derived nanoporous multifunctional fillers enhancing the performances of polymer electrolytes for solid-state lithium batteries. *Journal of Materials Chemistry A* **2019,** *7* (6), 2653-2659, DOI: 10.1039/c8ta10124h.

(4) Chen, L.; Li, Y.; Li, S.-P.; Fan, L.-Z.; Nan, C.-W.; Goodenough, J. B. PEO/garnet composite electrolytes for solid-state lithium batteries: From "ceramic-in-polymer" to "polymer-in-ceramic". *Nano Energy* **2018,** *46*, 176-184, DOI: 10.1016/j.nanoen.2017.12.037.

(5) Wang, Z.; Tan, R.; Wang, H.; Yang, L.; Hu, J.; Chen, H.; Pan, F. J. A. M. A Metal–Organic-Framework-Based Electrolyte with Nanowetted Interfaces for High-Energy-Density Solid-State Lithium Battery. **2018,** *30* (2), 1704436.

(6) Huo, H.; Zhao, N.; Sun, J.; Du, F.; Li, Y.; Guo, X. Composite electrolytes of polyethylene oxides/garnets interfacially wetted by ionic liquid for room-temperature solid-state lithium battery. *Journal of Power Sources* **2017,** *372*, 1-7, DOI: 10.1016/j.jpowsour.2017.10.059.

(7) Zhu, L.; Zhu, P. H.; Fang, Q. X.; Jing, M. X.; Shen, X. Q.; Yang, L. Z. A novel solid PEO/LLTO-nanowires polymer composite electrolyte for solid-state lithium-ion battery. *Electrochimica Acta* **2018,** *292*, 718-726, DOI: 10.1016/j.electacta.2018.10.005.

(8) He, Z. J.; Chen, L.; Zhang, B. C.; Liu, Y. C.; Fan, L. Z. Flexible poly(ethylene carbonate)/garnet composite solid electrolyte reinforced by poly(vinylidene fluoride-hexafluoropropylene) for lithium metal batteries. *Journal of Power Sources* **2018,** *392*, 232-238, DOI: 10.1016/j.jpowsour.2018.05.006.

(9) Chen, F.; Yang, D. J.; Zha, W. P.; Zhu, B. D.; Zhang, Y. H.; Li, J. Y.; Gu, Y. P.; Shen, Q.; Zhang, L. M.; Sadoway, D. R. Solid polymer electrolytes incorporating cubic $Li_7La_3Zr_2O_{12}$ for all-solid-state lithium rechargeable batteries. *Electrochimica Acta* **2017,** *258*, 1106-1114, DOI: 10.1016/j.electacta.2017.11.164.

(10) Duan, H.; Yin, Y. X.; Shi, Y.; Wang, P. F.; Zhang, X. D.; Yang, C. P.; Shi, J. L.; Wen, R.; Guo, Y. G.; Wan, L. J. Dendrite-Free Li-Metal Battery Enabled by a Thin Asymmetric Solid Electrolyte with Engineered Layers. *J Am Chem Soc* **2018,** *140* (1), 82-85, DOI: 10.1021/jacs.7b10864.

(11) Zhang, X.; Liu, T.; Zhang, S.; Huang, X.; Xu, B.; Lin, Y.; Xu, B.; Li, L.; Nan, C. W.; Shen, Y. Synergistic Coupling between $Li_{6.75}La_3Zr_{1.75}Ta_{0.25}O_{12}$ and Poly(vinylidene fluoride) Induces High Ionic Conductivity, Mechanical Strength, and Thermal Stability of Solid Composite Electrolytes. *J Am Chem Soc* **2017,** *139* (39), 13779-13785, DOI: 10.1021/jacs.7b06364.

(12) Duan, H.; Yin, Y.-X.; Zeng, X.-X.; Li, J.-Y.; Shi, J.-L.; Shi, Y.; Wen, R.; Guo, Y.-G.; Wan, L.-J. In-situ plasticized polymer electrolyte with double-network for flexible solid-state lithium-metal batteries. *Energy Storage Materials* **2018,** *10*, 85-91, DOI: 10.1016/j.ensm.2017.06.017.

(13) Zhang, W.; Nie, J.; Li, F.; Wang, Z. L.; Sun, C. A durable and safe solid-state lithium battery with a hybrid electrolyte membrane. *Nano Energy* **2018,** *45*, 413-419, DOI: 10.1016/j.nanoen.2018.01.028.

(14) Chen, L.; Li, W.; Fan, L. Z.; Nan, C. W.; Zhang, Q. J. A. F. M. Intercalated Electrolyte with High Transference Number for Dendrite-Free Solid-State Lithium Batteries. **2019**, 1901047.

(15) Zhang, J.; Zhao, N.; Zhang, M.; Li, Y.; Chu, P. K.; Guo, X.; Di, Z.; Wang, X.; Li, H. Flexible and

ion-conducting membrane electrolytes for solid-state lithium batteries: Dispersion of garnet nanoparticles in insulating polyethylene oxide. *Nano Energy* **2016,** *28*, 447-454, DOI: 10.1016/j.nanoen.2016.09.002.

(16) Huo, H.; Chen, Y.; Luo, J.; Yang, X.; Guo, X.; Sun, X. Rational Design of Hierarchical "Ceramic-in-Polymer" and "Polymer-in-Ceramic" Electrolytes for Dendrite-Free Solid-State Batteries. *Advanced Energy Materials* **2019**, DOI: 10.1002/aenm.201804004.